RSC Advances

ROYAL SOCIETY OF CHEMISTRY

www.rsc.org/advances

Luminescence and energy transfer of 432 nm blue LED radiation-converting phosphor $Ca_4Y_6O(SiO_4)_6:Eu^{2+}$, Mn^{2+} for warm white LEDs

Panlai Li*, Zhijun Wang*, Qinglin Guo, Zhiping Yang

Hebei Key Lab of Optic-electronic Information and Materials, College of Physics Science & Technology, Hebei University, Baoding 071002, China

Abstract: A series of $Ca_4Y_6O(SiO_4)_6:Eu^{2+}$, Mn^{2+} phosphors are synthesized by a solid state method. $Ca_4Y_6O(SiO_4)_6:Eu^{2+}$, Mn^{2+} can be excited at wavelength ranging from 250 to 500 nm, which is well matched with ultraviolet-visible light emitting diode. Under 432 nm excitation, $Ca_4Y_6O(SiO_4)_6:Eu^{2+}$, Mn^{2+} can create warm white emission by energy transfer from Eu^{2+} to Mn^{2+}. A warm white light emitting diode is fabricated by combining a 432 nm blue LED with a single phase warm white emitting phosphor $Ca_{3.92}Y_6O(SiO_4)_6:0.05Eu^{2+}$, $0.03Mn^{2+}$, which has CIE chromaticity coordinates (0.336, 0.319), correlated color temperature (CCT) 4326K and color rendering index (R_a) 86, respectively. The results indicate $Ca_4Y_6O(SiO_4)_6:Eu^{2+}$, Mn^{2+} may serve as potential warm white emitting phosphor for blue LED based white LEDs.

Keywords: Luminescence; Energy transfer; $Ca_4Y_6O(SiO_4)_6:Eu^{2+}$, Mn^{2+}; Light-emitting diodes

1. Introduction

White light emitting diodes (LEDs) are mainstream in solid-state lighting because of several advantages, such as energy saving, no mercury pollution, long life, short response time, small size, good hardness and high energy efficiency.[1-3] White LEDs could be fabricated by blue chip-pumped yellow YAG:Ce^{3+}, whereas color rendering index (CRI) of white light made by the complementary blue and yellow emission is deficient due to the lack of red light contribution.[4] Therefore, several red

*li_panlai@126.com
*wangzj1998@126.com

emitting phosphors are developed to add into YAG:Ce^{3+} to offset the deficiency.[5] Unfortunately, the extreme difference in degradation between different host phosphors will produce color aberration. In order to avoid the problem, design of single-phase phosphor pumped by ultraviolet (UV) or near-UV chips is of significance for white LEDs because single-phase phosphor has advantages of excellent color rendering indexes, and electro-optical design is simple to control different colors in comparison with mixed phosphors.[6-13] Although the UV or near-UV chip is available, however, the efficiency of these chips is still obviously lower than that of blue chip. Accordingly, it is important to explore the single phase phosphor with green-to-red emission bands for blue LEDs.[14] A phosphor could emit a couple of radiation by co-doped activators with f-f or d-d electron configurations, such as Eu^{2+}/Mn^{2+}, Ce^{3+}/Mn^{2+} and Ce^{3+}/Eu^{2+}, energy transfer would occur between activator/co-activator couples by effective resonant type via a multipolar interaction and the energy transfer to Mn^{2+} can be of exchange interaction.[6-13, 15-17] Nevertheless, as far as we know, codoped single-phase phosphors with blue absorption or for blue LEDs were rarely investigated.[14] Moreover, for indoor illumination, warm white light which can be used for indoor illumination, similar to most luminescence lamps, CCT (CCT≤4500 K or even CCT≤3500 K), is more favorable for human sight and more recommended.[18-20] Therefore, it is urgent to search for novel and highly efficient warm white emitting phosphor that can be excited by blue LEDs.

Ternary rare-earth-metal silicate $Ca_4Y_6O(SiO_4)_6$ is an efficient host lattice for the luminescence of various rare earth ions and mercury-like ions.[21, 22] The oxy-apatite host lattice consists of two cationic sites, that is, the 9-fold coordinated 4f sites with C_3 point symmetry and 7-fold coordinated 6h sites with C_s point symmetry. Both sites are suitable and easily accommodate a great variety of rare earth and transitional-metal ions.[23] Luminescent properties of Sb^{3+}, Pb^{2+}, Eu^{3+}, Tb^{3+} and Dy^{3+} in

$Ca_4Y_6O(SiO_4)_6$ are reported.[21, 22, 24,25] Moreover, Lin et al. explored white emission properties of $Ca_4Y_6O(SiO_4)_6$:Ce^{3+}/Tb^{3+}/Mn^{2+}, which can be effectively excited by 284 and 358 nm UV radiation excitation.[23] Nonetheless, $Ca_4Y_6O(SiO_4)_6$:Ce^{3+}/Tb^{3+}/Mn^{2+} has a low absorption in the blue region. Therefore, in the present work, a warm white emitting phosphor $Ca_4Y_6O(SiO_4)_6$:Eu^{2+}, Mn^{2+} which can be excited by blue light is explored, and energy transfer property from Eu^{2+} to Mn^{2+} is studied.

2. Experimental section

2.1. Sample preparation

A series of $Ca_{4-x-y}Y_6O(SiO_4)_6$:xEu^{2+}, yMn^{2+} (x, y: mole concentration) samples are synthesized by a high temperature solid state method. Initial materials $CaCO_3$ (A.R.), Y_2O_3 (A.R.), SiO_2 (A.R.), $MnCO_3$ (99.99%) and Eu_2O_3 (99.99%) are weighted in stoichiometric proportion, thoroughly mixed and ground by an agate mortar and pestle for more than 30 min till they are uniformly distributed. The obtained mixtures are heated at 900 ℃ for 2 h in crucibles along with an atmosphere. After that, the samples are thoroughly ground and sintered at 1350 ℃ for 4 h with a reducing atmosphere ($5\%H_2/95\%N_2$), then slowly cooled down to room temperature. In order to measure characteristics, the samples are ground into powder.

2.2. Materials characterization

Phase formation is determined by X-ray diffraction (XRD) in a Bruker AXS D8 advanced automatic diffractometer (Bruker Co., German) with Ni-filtered Cu Kα1 radiation (λ=0.15406 nm), and a scan rate of 0.02°/s is applied to record the patterns in the 2θ range from 10° to 60°. Steady time resolved photoluminescence spectra are detected by a FLS920 fluorescence spectrometer, and the exciting sources are a 450 W Xe lamp. Curve fittings are performed on the luminescence decay curves to confirm the decay time. Commission International de I'Eclairage (CIE) chromaticity

coordinates are measured by a PMS-80 spectra analysis system. Quantum efficiency is analyzed with a photoluminescence quantum efficiency measurement system (C9920-02, Hamamatsu Photonics, Shizuoka) containing a 150 W xenon lamp. All measurements are carried out at room temperature. High-temperature photoluminescence spectra are detected by a fluorescence spectrophotometer (Hitachi F-4600) with a TAP-02 high temperature control system, the scanning wavelength range from 400 to 700 nm, a spectral resolution is 0.2 nm, and the exciting source is a 450 W Xe lamp.

3. Results and discussion

3.1. Phase formation

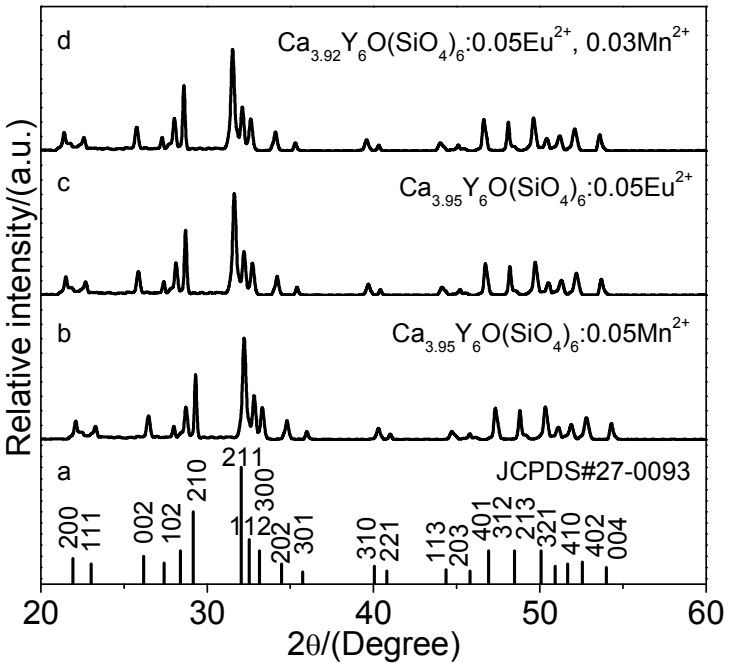

Fig.1. XRD patterns of $Ca_{3.95}Y_6O(SiO_4)_6$:0.05Eu^{2+}, $Ca_{3.95}Y_6O(SiO_4)_6$:0.05Mn^{2+} and $Ca_{3.92}Y_6O(SiO_4)_6$:0.05Eu^{2+}, 0.03Mn^{2+} with the standard data of $Ca_4Y_6O(SiO_4)_6$ (JCPDS No.27-0093).

XRD patterns of $Ca_{4-x-y}Y_6O(SiO_4)_6$:$x$$Eu^{2+}$, $y$$Mn^{2+}$ are recorded and a similar diffraction patterns are observed for each sample. As a representative, the XRD patterns of $Ca_{3.95}Y_6O(SiO_4)_6$:0.05Eu^{2+}, $Ca_{3.95}Y_6O(SiO_4)_6$:0.05Mn^{2+} and $Ca_{3.92}Y_6O(SiO_4)_6$:0.05Eu^{2+}, 0.03Mn^{2+} are shown in Fig.1. When

compared the diffraction data with the standard JCPDS card (No.27-0093), and there is no difference between the doped impurity $Ca_4Y_6O(SiO_4)_6$ and $Ca_4Y_6O(SiO_4)_6$. The uniform diffraction patterns indicate that the phase formation of $Ca_4Y_6O(SiO_4)_6$ is not influenced by a little amounts of Eu^{2+}, Mn^{2+} and Eu^{2+}/Mn^{2+}. $Ca_4Y_6O(SiO_4)_6$ has a hexagonal crystal structure, with a space group $P6_3/m(176)$, the cell parameters a=b=0.9356 nm, c=0.6793 nm, α=β=90°, and γ=120°. However, as shown in Fig.S1, it is noted that the diffraction peaks (2θ) shift slightly to small (Eu^{2+}) or large (Mn^{2+}) degree comparing with those of standard PDF card, which mean the diversification of lattice parameters. According to equation of $1/d^2=(h^2+k^2+l^2)/a^2$, the lattice constant a can be achieved. For $Ca_{3.95}Y_6O(SiO_4)_6$:0.05Mn^{2+} and $Ca_{3.95}Y_6O(SiO_4)_6$:0.05Eu^{2+}, the a values are calculated to be 0.9317 nm and 0.9396 nm, respectively. The values which are a little smaller (or bigger) than that (a=0.9356 nm) of blank hexagonal $Ca_4Y_6O(SiO_4)_6$ phase. The contraction maybe attribute to the ionic radius of replacement ions is smaller than that of host ions, whereas the expansion may due to the ionic radius of replacement ions is larger than that of host ions. Therefore, in view of the similar ion radius and valence, Eu^{2+} (0.130 nm) ions are expected to substitute of Ca^{2+} (0.118 nm) sites in the compound $Ca_4Y_6O(SiO_4)_6$.[26] According to the same principle and Ref [23], Ca^{2+} sites are expected to be replaced by Mn^{2+} (0.090 nm) ions in the same crystal structure.

3.2. Photoluminescence properties

Fig.2(a) shows that $Ca_{3.95}Y_6O(SiO_4)_6$:0.05Eu^{2+} has green emission under 380 nm and 432 nm excitation. Monitored at 527 nm, excitation spectrum of $Ca_4Y_6O(SiO_4)_6$:Eu^{2+} has two obvious excitation bands, which are mainly due to the transitions of Eu^{2+} from $4f^7$ ground state to $4f^65d^1$ excited state.[7, 8] Eu^{2+} ions have many excited states, and consequently, they show unresolved broad excitation spectrum. The excitation spectrum shows that excitation wavelength can extend from 250

to 500 nm, though the peak locates at 380 nm, however, there is an obvious excitation intensity in the blue region (such as 432 nm). As shown in Fig.2(a), obviously, $Ca_4Y_6O(SiO_4)_6:Eu^{2+}$ can be effectively excited by 432 nm blue light, and produce green emission. Inset of Fig.2(a) shows that emission intensities of $Ca_4Y_6O(SiO_4)_6:Eu^{2+}$ enhance with increase Eu^{2+} concentration, then decrease with further increase Eu^{2+} concentration, and the optimal Eu^{2+} concentration is x=0.05.

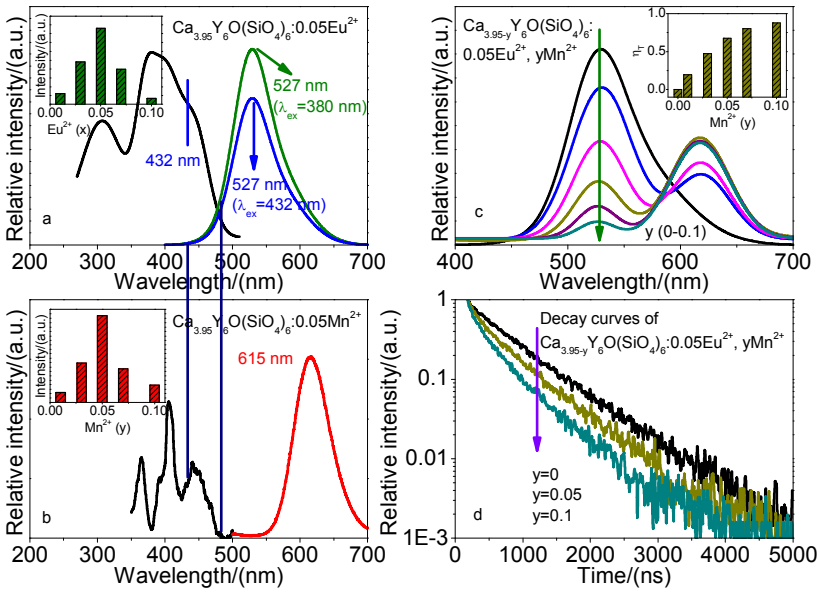

Fig.2. (a) Emission and excitation spectra of $Ca_{3.95}Y_6O(SiO_4)_6:0.05Eu^{2+}$ (λ_{ex}=380 nm, 432 nm; λ_{em}=527 nm);

(b) Emission and excitation spectra of $Ca_{3.95}Y_6O(SiO_4)_6:0.05Mn^{2+}$ (λ_{ex}=405 nm; λ_{em}=615 nm);

(c) Emission spectra of $Ca_{3.95-y}Y_6O(SiO_4)_6:0.05Eu^{2+}$, $y$$Mn^{2+}$ (λ_{ex}=432 nm);

(d) Decay curves of $Ca_{3.95-y}Y_6O(SiO_4)_6:0.05Eu^{2+}$, $y$$Mn^{2+}$ (λ_{ex}=432 nm).

Inset: Emission intensities ((a)Eu^{2+} and (b) Mn^{2+}) and (c) η_Γ as a function of impurity concentration.

Fig.2(b) shows typical emission and excitation spectra of $Ca_{3.95}Y_6O(SiO_4)_6:0.05Mn^{2+}$ under 405 nm excitation. As well know, *d-d* transitions of Mn^{2+} are spin and parity forbidden transition, thus for Mn^{2+} doped $Ca_4Y_6O(SiO_4)_6$, its excitation transition is difficult to be pumped and emission intensity is very weak. A broad emission band peaked at 615 nm is attributed to the spin-forbidden

$^4T_1(4G)$-$^6A_1(6S)$ transition. Its excitation spectrum consists of several bands peaked at 365, 405, and 441 nm corresponding to the transitions from $^6A_1(6S)$ to $^4T_2(^4D)$, [$^4A_1(^4G)$, $^4E(^4G)$] and $^4T_2(^4G)$, respectively.[7-10] Inset of Fig.2(b) shows that the Mn^{2+} optimal concentration is y=0.05.

As shown in Fig.2(a) and (b), there is a spectral overlap between the emission band of $Ca_4Y_6O(SiO_4)_6$:Eu^{2+} and the excitation band of $Ca_4Y_6O(SiO_4)_6$:Mn^{2+}. Accordingly, an energy transfer from Eu^{2+} to Mn^{2+} is expected in $Ca_4Y_6O(SiO_4)_6$. Under 432 nm excitation, emission spectra of $Ca_{3.95-y}Y_6O(SiO_4)_6$:0.05Eu^{2+}, $y$$Mn^{2+}$ with increase Mn^{2+} concentration are measured, and the variation in emission spectra and emission intensity of samples are shown in Fig.2(c). The results show that the emission intensity of Mn^{2+} is observed to increase systematically from y=0.01-0.05, and reach saturation as y equal to or larger than 0.05. In other words, there is an energy transfer from Eu^{2+} to Mn^{2+} in $Ca_4Y_6O(SiO_4)_6$. In order to well understand the energy transfer process, energy transfer efficiency (η_T) from Eu^{2+} to Mn^{2+} of samples is calculated. The η_T from Eu^{2+} to Mn^{2+} can be expressed according to Paulose et al.[27]

$$\eta_T=1-(I_S/I_{S0}) \quad (1)$$

where I_{S0} and I_S are luminescent intensities of sensitizer Eu^{2+} in the absence and presence of activator Mn^{2+}. As a result, the η_T values from Eu^{2+} to Mn^{2+} for $Ca_{3.95-y}Y_6O(SiO_4)_6$:0.05Eu^{2+}, $y$$Mn^{2+}$ ($0\leq y\leq 0.1$) are calculated and shown in the inset of Fig.2(c), and the η_T is found to increase gradually with increase Mn^{2+} concentration. The results mean that the energy transfer from Eu^{2+} to Mn^{2+} exists in $Ca_4Y_6O(SiO_4)_6$:Eu^{2+}, Mn^{2+}.

It is known that if energy is transferred from a donor to an acceptor, the temporal decay of donor decreases. Montoired at 527 nm emission, the temporal decay of Eu^{2+} as a function of Mn^{2+} concentration is investigated, and the results are shown in Fig.2(d). For Eu^{2+} and Mn^{2+} co-doped

samples, if Eu^{2+} and Mn^{2+} work independently, and there is no energy transfer between them, the photoluminescence lifetime of both activators will be as same as in the single-doped samples. If energy transfer from Eu^{2+} to Mn^{2+} exists in $Ca_4Y_6O(SiO_4)_6$, the decay of Eu^{2+} excitation state will be accelerated by this energy transfer channel, and consequently the lifetime of Eu^{2+} will be shortened. As shown in Fig.2(d), the shorten of the lifetime of Eu^{2+} confirmed the energy transfer between Eu^{2+} and Mn^{2+} ions. In other words, the energy transfer of $Eu^{2+}\rightarrow Mn^{2+}$ exists in $Ca_4Y_6O(SiO_4)_6$.

Generally, there is two aspects to be responsible for resonant energy-transfer mechanism: one is exchange interaction and the other is multipolar interaction. It is well known that if energy transfer results from the exchange interaction, critical distance between sensitizer and activator should be shorter than 5 Å. In many cases, concentration quenching is due to energy transfer from one activator to another until an energy sink in the lattice is reached. The critical distance (R_c) for energy transfer from Eu^{2+} to Mn^{2+} ions can be calculated using concentration quenching method, and the critical distance $R_{Eu\text{-}Mn}$ between Eu^{2+} and Mn^{2+} can be estimated by[28]

$$R_{Eu\text{-}Mn}=2[3V/(4\pi x_c N)]^{1/3} \quad (2)$$

where x_c is the total concentration of Eu^{2+} and Mn^{2+}, N is number of Z ions in the unit cell (for $Ca_4Y_6O(SiO_4)_6$, N=10), and V is volume of the unit cell (for $Ca_4Y_6O(SiO_4)_6$, V=514.96 $Å^3$). The estimated distance ($R_{Eu\text{-}Mn}$) for $Ca_{3.95-y}Y_6O(SiO_4)_6$:0.05Eu^{2+}, $y$$Mn^{2+}$ phosphors (x_c=0.05, 0.06, 0.08, 0.10, 0.12, and 0.15) are 12.53, 11.79, 10.71, 9.94, 9.36 and 8.69 Å, respectively. The distances between Eu^{2+} and Mn^{2+} become shorter with increase Mn^{2+} concentration. x is critical concentration at which the emission intensity of donor (Eu^{2+}) in the presence of acceptor (Mn^{2+}) is half that in the absence of the acceptor (Mn^{2+}). Therefore, the critical distance (R_c) of energy transfer is calculated to be about 10.71 Å for $Ca_{3.95-y}Y_6O(SiO_4)_6$:0.05Eu^{2+}, $y$$Mn^{2+}$. $R_{Eu\text{-}Mn}$ for various Eu^{2+} content levels is

much larger than the typical critical distance for exchange interaction (5 Å).[29] The results indicate that little possibility of energy transfer via the exchange interaction mechanism. Thus, the electric multipolar interaction may take place for energy transfer between the Eu^{2+} and Mn^{2+} ions.

On the basis of Dexter's energy transfer formula for exchange and multipolar interactions, the following relation can be obtained[30-35]

$$\ln(\eta_0/\eta) \propto C \quad (3)$$

$$(\eta_0/\eta) \propto C^{\alpha/3} \quad (4)$$

where η_0 and η are luminescence quantum efficiency of Eu^{2+} in the absence and presence of Mn^{2+}, respectively; C is the total concentration of Eu^{2+} and Mn^{2+}. Eq.3 corresponds to exchange interaction, and Eq.4 with α=6, 8, 10 is ascribed to dipole-dipole, dipole-quadrupole, and quadrupole-quadrupole interactions, respectively.

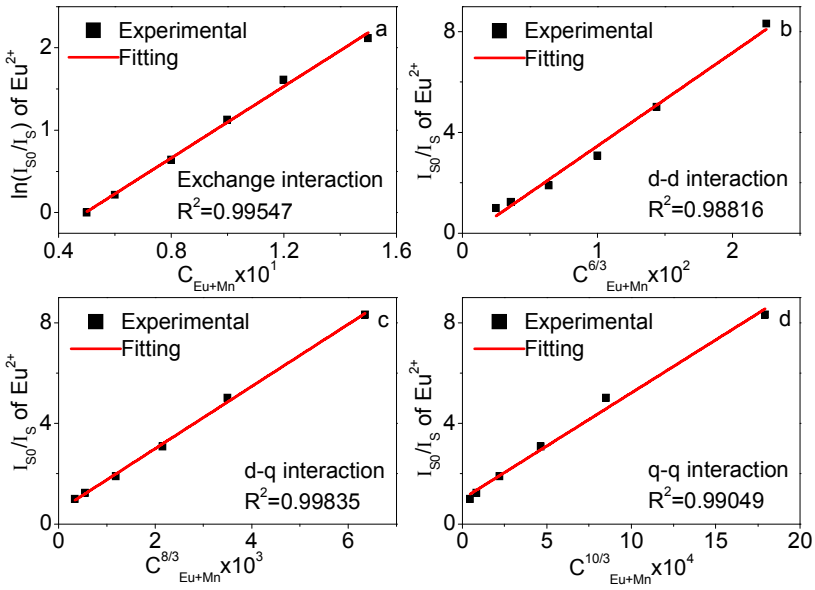

Fig.3. Dependence of $\ln(I_{S0}/I_S)$ of Eu^{2+} on (a) C and I_{S0}/I_S of Eu^{2+} (b) $C^{6/3}$, (c) $C^{8/3}$, and (d) $C^{10/3}$.

The relationships of $\ln(I_{S0}/I_S) \propto C$ and $(I_{S0}/I_S) \propto C^{\alpha/3}$ are illustrated in Fig.3. By consulting the fitting factor R, the relation $(I_{S0}/I_S) \propto C^{8/3}$ has the best fitting, implying that the dipole-quadrupole

interaction is applied for the energy transfer from Eu^{2+} to Mn^{2+}. The results also prove the conclusion using the critical distance (R_c) of energy transfer.

For white LEDs application, quantum efficiency (QE) is an important parameter for phosphors. Tunable white light emission with suitable QE can be obtained in $Ca_{3.95-y}Y_6O(SiO_4)_6$:$0.05Eu^{2+}$, yMn^{2+} by the energy transfer from Eu^{2+} to Mn^{2+} ions, as shown in Table 1. For warm white light emitting phosphor $Ca_{3.95-y}Y_6O(SiO_4)_6$:$0.05Eu^{2+}$, yMn^{2+}, the QE can reach 39.6%. The data indicate that $Ca_{3.95-y}Y_6O(SiO_4)_6$:$0.05Eu^{2+}$, yMn^{2+} has relatively appropriate QE and warm white light emission, therefore, it could be used as phosphor for white LEDs.

Table 1. CIE chromaticity coordinates (X, Y), CCT (K) and quantum efficiency (QE) for $Ca_{3.95-y}Y_6O(SiO_4)_6$:$0.05Eu^{2+}$, yMn^{2+} (λ_{ex}=432 nm).

Samples	CIE coordinates (X, Y)	CCT (K)	Quantum efficiency (QE)
y=0	(0.306, 0.502)	7119	37.1%
y=0.01	(0.319, 0.436)	5619	38.3%
y=0.03	(0.336, 0.319)	4326	39.6%
y=0.05	(0.356, 0.313)	3601	39.1%
y=0.07	(0.438, 0.335)	3209	38.3%
y=0.1	(0.581, 0.366)	2653	38.1%

Color coordinates are one of the important factors for evaluating the performance of phosphors. As shown in Table 1, Commission Internationale de I'Eclairage (CIE 1931) chromaticity coordinates and CCT of $Ca_{3.95-y}Y_6O(SiO_4)_6$:$0.05Eu^{2+}$, yMn^{2+} are measured. Eu^{2+} concentration is fixed at 0.05 as the concentration of Mn^{2+} increases from 0 to 0.1, the corresponding color of phosphor shifts from green to white light, then to red. In particular, CCT of white light can also be tuned by appropriately

tuning Mn^{2+} concentration. It is clear that warm white light can be created for different practical application by varying Mn^{2+} concentration in $Ca_{3.95-y}Y_6O(SiO_4)_6$:0.05Eu^{2+}, $y$$Mn^{2+}$.

For application of high power LEDs, thermal stability of sample is one of the important issues to be considered. For $Ca_{3.92}Y_6O(SiO_4)_6$:0.05Eu^{2+}, 0.03Mn^{2+}, Fig.4 shows temperature dependence of emission spectra under 432 nm excitation. The inset shows temperature quenching characteristics of commercial YAG:Ce and $Ca_{3.92}Y_6O(SiO_4)_6$:0.05Eu^{2+}, 0.03Mn^{2+} in the temperature range from 25 to 250 ℃. Compared with YAG:Ce, the emission intensity of $Ca_{3.92}Y_6O(SiO_4)_6$:0.05Eu^{2+}, 0.03Mn^{2+} is very close to that of YAG:Ce when the temperature is raised up to 200 ℃, for example, the intensity of sample drops to about 81% when the temperature is 200 ℃, while that of YAG:Ce decreases to 83% of the initial value. The results indicate that the sample has good thermal quenching properties.

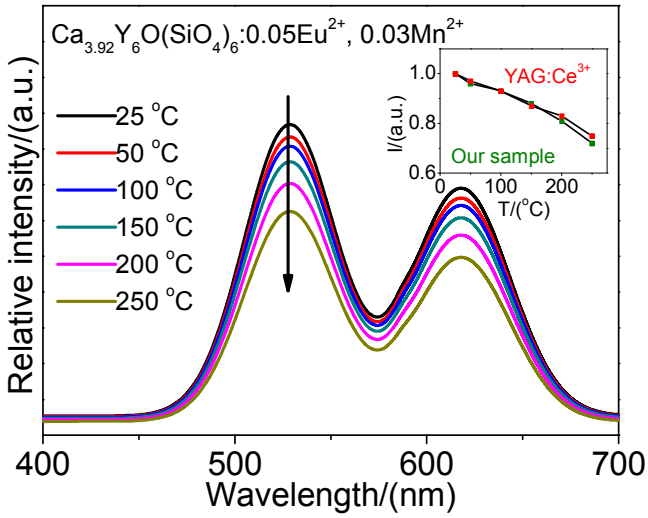

Fig.4. Temperature dependent emission spectra of $Ca_{3.92}Y_6O(SiO_4)_6$:0.05Eu^{2+}, 0.03Mn^{2+} (λ_{ex}=432 nm).

Inset: normalized intensity of $Ca_{3.92}Y_6O(SiO_4)_6$:0.05Eu^{2+}, 0.03Mn^{2+} and YAG:Ce as a function of temperature.

To further understand the temperature dependence, Arrhenius fitting following the below equation was conducted[36]

$$I_T=I_0/[1+c\exp(-\Delta E/kT)] \quad (5)$$

where I_0 is the initial emission intensity of phosphor at room temperature, I_T is the emission intensity at T K, c is a constant, ΔE is the activation energy for thermal quenching, and k is the Boltzmann constant (8.617×10^{-5} eV). The fitting result is shown in Fig.5 and activation energy ΔE is achieved as 0.162 eV. The relatively high activation energy indicates that $Ca_4Y_6O(SiO_4)_6$:Eu^{2+}, Mn^{2+} has good thermal stability, and may be applied for high-powered LED application.

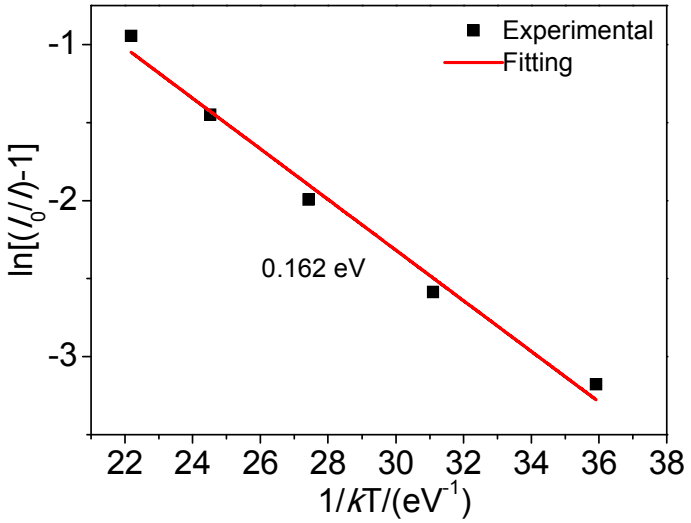

Fig.5. Arrhenius fitting of emission intensity of $Ca_{3.92}Y_6O(SiO_4)_6$:$0.05Eu^{2+}$, $0.03Mn^{2+}$ and the calculated activation energy (ΔE) for thermal quenching.

3.3. Application of $Ca_4Y_6O(SiO_4)_6$:Eu^{2+}, Mn^{2+}

To demonstrate application of $Ca_4Y_6O(SiO_4)_6$:Eu^{2+}, Mn^{2+}, a white LED is fabricated by coating $Ca_{3.92}Y_6O(SiO_4)_6$:$0.05Eu^{2+}$, $0.03Mn^{2+}$ phosphor on a 432 nm UV-chip that is driven by a 20 mA current. Fig.6 shows emission spectrum of white LEDs, which has CIE chromaticity coordinates (0.336, 0.319) and correlated color temperature (CCT) 4326K, and color rendering index (R_a) 86, respectively. Obviously, performance of white LEDs based on $Ca_{3.92}Y_6O(SiO_4)_6$:$0.05Eu^{2+}$, $0.03Mn^{2+}$ is superior to white LEDs that are fabricated by coating YAG:Ce yellow phosphor on blue chips [(0.292, 0.325), CCT=7756 K] because the former shows higher color rendering index and lower

CCT value.[4] Moreover, Table S1 depicts the CIE chromaticity coordinates and correlated color temperature of $Ca_{3.92}Y_6O(SiO_4)_6$:0.05Eu^{2+}, 0.03Mn^{2+} sample in white LEDs device with the current (20-200 mA). The results show that the white LEDs have a relatively appropriate color stability.

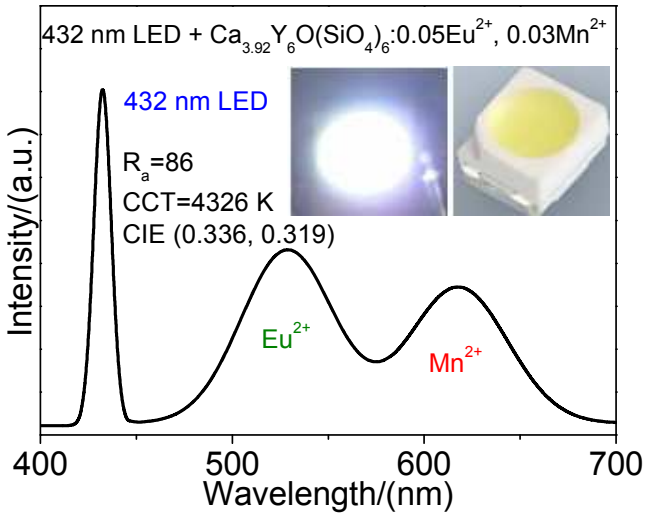

Fig.6. Emission spectrum of a pc-LED lamp fabricated with a 432 nm LED chip and warm white emitting phosphor $Ca_{3.92}Y_6O(SiO_4)_6$:0.05Eu^{2+}, 0.03Mn^{2+}. Inset shows appearance of a well-packaged trichromatic LED lamp in operation.

4. Conclusion

In summary, $Ca_4Y_6O(SiO_4)_6$:Eu^{2+}, Mn^{2+} can be effectively excited by 432 nm blue LED, and produce warm white emission by the energy transfer from Eu^{2+} to Mn^{2+}, and the QE is about 39.6%. A warm white light emitting diode is fabricated by combining a 432 nm blue LED with the warm white emitting phosphor $Ca_{3.92}Y_6O(SiO_4)_6$:0.05Eu^{2+}, 0.03Mn^{2+}. The white LEDs have CIE coordinates (0.336, 0.319), correlated color temperature (CCT) 4326K and color rendering index (R_a) 86, respectively. The results indicate that $Ca_4Y_6O(SiO_4)_6$:Eu^{2+}, Mn^{2+} may be a potential single-phase white emitting phosphor for blue based LEDs.

Acknowledgments

The work is supported by the National Natural Science Foundation of China (No. 50902042), the Natural Science Foundation of Hebei Province, China (No.A2014201035; E2014201037) and the Education Office Research Foundation of Hebei Province, China (Nos.ZD2014036; QN2014085).

References

1 M. Shang, C. Li and J. Lin. Chem. Soc. Rev., 2014, 43, 1372-1386.

2 S. Ye, F. Xiao, Y. X. Pan, Y. Y. Ma and Q. Y. Zhang. Mater. Sci. Eng. R, 2010, 71, 1-34.

3 C. C. Lin and R.-S. Liu. J. Phys. Chem. Lett., 2011, 2, 1268-1277.

4 C.-W. Yeh, W.-T. Chen, R.-S. Liu, S.-F. Hu, H.-S. Sheu, J.-M. Chen and H. T. Hintzen. J. Am. Chem. Soc., 2012, 134, 14108-14117.

5 S. E. Brinkley, N. Pfaff, K. A. Denault, Z. Zhang, H. T. (Bert) Hintzen, R. Seshadri, S. Nakamura and S. P. DenBaars. Appl. Phys. Lett., 2011, 99, 241106.

6 K. Li, D. Geng, M. Shang, Y. Zhang, H. Lian and J. Lin. J. Phys. Chem. C, 2014, 118, 11026-11034.

7 Y. Chen, Y. Li, J. Wang, M. Wu and C. Wang. J. Phys. Chem. C, 2014, 118, 12494-12499.

8 Y. Li, Y. Shi, G. Zhu, Q. Wu, H. Li, X. Wang, Q. Wang and Y. Wang. Inorg. Chem., 2014, 53, 7688-7675.

9 N. Guo, H. You, C. Jia, R. Ouyang and D. Wu. Dalton Trans., 2014, 43, 12373-12379.

10 C.-K. Chang and T.-M. Chen. Appl. Phys. Lett., 2007, 91, 081902.

11 C.-H. Huang, W.-R. Liu and T.-M. Chen. J. Phys. Chem. C, 2010, 114, 18698-18701.

12 G. Li, D. Geng, M. Shang, C. Peng, Z. Cheng and J. Lin. J. Mater. Chem., 2011, 21, 13334-13344.

13 P. Li, Z. Wang, Z. Yang and Q. Guo. J. Mater. Chem. C, 2014, 2, 7823-7829.

14 W.-J. Yang and T.-M. Chen. Appl. Phys. Lett., 2007, 90, 171908.

15 D. Geng, M. Shang, Y. Zhang, H. Lian and J. Lin. Dalton Trans., 2013, 42, 15372-15380.

16 M. Jiao, Y. Jia, W. Lü, W. Lv, Q. Zhao, B. Shao and H. You. J. Mater. Chem. C, 2014, 2, 90-97.

17 M. Shang, D. Geng, Y. Zhang, G. Li, D. Yang, X. Kang and J. Lin. J. Mater. Chem., 2012, 22, 19094-19104.

18 N. Guo, Y. Zheng, Y. Jia, H. Qiao and H. You. J. Phys. Chem. C, 2012, 116, 1329-1334.

19 Z. Wang, P. Li, Q. Guo and Z. Yang. Mater. Res. Bull., 2014, 52, 30-36.

20 G. Zhu, S. Xin, Y. Wen, Q. Wang, M. Que and Y. Wang. RSC Adv., 2013, 3, 9311-9318.

21 J. Lin and Q. Su. J. Mater. Chem., 1995, 5, 603-606.

22 W. L. Wanmaker, J. W. ter Vrugt and J. G. Verlijsdonk. J. Solid State Chem., 1971, 3, 452-457.

23 G. Li, Y. Zhang, D. Geng, M. Shang, C. Peng, Z. Cheng and J. Lin. ACS Appl. Mater. Interfaces, 2012, 4, 296-305.

24 M. J. Lammers and G. Blasse. J. Electrochem. Soc., 1987, 134, 2068-2072.

25 J. P. M. van Vliet and G. Blasse. Mater. Res. Bull., 1990, 25, 391-394.

26 C.-H. Huang, Y.-C. Chen, T.-M. Chen, T.-S. Chan and H.-S. Sheu. J. Mater. Chem., 2011, 21, 5645-5649.

27 P. I. Paulose, G. Jose, V. Thomas, N. V. Unnikrishnan and M. K. R. Warrier. J. Phys. Chem. Solids, 2003, 64, 841-846.

28 G. Blass. Philips Res. Rep., 1969, 24, 131-144.

29 G. Blasse and B. C. Grabmaier. Luminescent Materials, Berlin: Springer, 1994.

30 D. L. Dexter and J. H. Schulman. J. Chem. Phys., 1954, 22, 1063-1070.

31 N. Guo, Y. Huang, H. You, M. Yang, Y. Song, K. Liu and Y. Zheng. Inorg. Chem., 2010, 49,

10907-10913.

32 R. Reisfeld, E. Greenberg, R. Velapoldi and B. Barnett. J. Chem. Phys., 1972, 56, 1698-1705.

33 U. Caldiño, J. L. Hernández-Pozos, C. Flores, A. Speghini and M. Bettinelli. J. Phys.: Condens. Matter, 2005, 17, 7297-7306.

34 R. Martínez-Martínez, M. García, A. Speghini, M. Bettinelli, C. Falcony and U. Caldiño. J. Phys.: Condens. Matter, 2008, 20, 395205.

35 C.-H. Huang, T.-W. Kuo and T.-M. Chen. ACS Appl. Mater. Interfaces, 2010, 2, 1395-1399.

36 P. Dorenbos. J. Phys.: Condens. Mater, 2005, 17, 8103-8111.